Acupuncture and Herbal Medicine

Celastrol promotes apoptosis of breast cancer MDA-MB-231 cells by targeting HSDL2

Li Liu[1], Yanqing Liu[2], Shujie Zhang[2], Junzhe Zhang[2], Yuqing Meng[2], Dandan Liu[2], Liwei Gu[2], Ying Zhang[2], Liting Xu[2], Ziyue Zhang[2], Minghong Zhao[1], Yinkwan Wong[3], Qixin Wang[2], Yongping Zhu[2,*], Jigang Wang[1,2,3,*]

[1]College of Pharmacy, Gannan Medical University, Ganzhou, China; [2]State Key Laboratory for Quality Ensurance and Sustainable Use of Dao-di Herbs, Artemisinin Research Center, and Institute of Chinese Materia Medica, China Academy of Chinese Medical Sciences, Beijing, China; [3]Department of Pharmacological Sciences, Yong Loo Lin School of Medicine, National University of Singapore, Singapore, Singapore

Abstract

Objective: Celastrol is a pentacyclic triterpenoid extracted from the traditional Chinese medicinal herb, *Tripterygium wilfordii*. This study aims to provide a scientific basis for the rational development and use of celastrol in breast cancer.

Method: A quantitative chemical biology approach was used to investigate the protein targets and molecular mechanisms of celastrol in breast cancer cells.

Results: Low-concentration celastrol exerted an anti-tumor effect by directly binding to hydroxysteroid dehydrogenase-like 2 (HSDL2) and inhibiting its expression. Moreover, the expression of the pro-apoptotic protein, Bcl-2-associated X (BaX), increased, the level of the anti-apoptotic protein, B-cell lymphoma-2 (Bcl-2), decreased, and the rate of apoptosis increased. After the transfection of cells with si-HSDL2, the apoptosis rate was similar to that observed after the administration of celastrol. However, apoptosis was reversed by the overexpression of HSDL2. Furthermore, our mass spectrometry (MS) data indicated a relationship between HSDL2 and the mitogen-activated protein kinase (MAPK) signaling pathway. We also found that the expression of HSDL2 was directly related to the degree of extracellular signal-regulated kinase (ERK) phosphorylation.

Conclusion: Celastrol may promote apoptosis by suppressing the HSDL2/MAPK/ERK signaling pathway.

Keywords: Activity-based protein profiling, Apoptosis, Celastrol, HSDL2.

Graphical abstract: http://links.lww.com/AHM/A99.

Introduction

Breast cancer is one of the most common types of cancer that threatens women's health[1]. According to data, the prevalence of breast cancer among Asian women was 22.9% in 2020[2], particularly in Nepal, a developing country[3]. Triple-negative breast cancer (TNBC) is a heterogeneous group of breast tumors defined by the absence of human epidermal growth factor receptor 2 (HER2), progesterone receptor (PR), and estrogen receptor (ER)[4]. Compared with other types of breast cancer, TNBC is characterized by strong invasiveness, highly difficult diagnosis, high metastatic potential, and poor effects of endocrine and targeted therapies[5]. Therefore, the development of new therapeutic strategies for TNBC is urgently required. In this study, we aims to explore the drug targets and their underlying mechanisms in MDA-MB-231 cells, a typical human TNBC cell line, to identify more efficient targets for TNBC treatment.

Celastrol is a pentacyclic triterpenoid extracted from the traditional Chinese medicinal herb *Tripterygium wilfordii*[6]. The pharmacological properties of celastrol, including anti-inflammatory[7], anti-obesity[8], antidepressant[9], and anti-cancer activities[10], have been extensively studied. Celastrol inhibits the proliferation and metastasis of various human tumor types, including gastric[11], liver[12], cervical[13], and breast cancers[14]. Studies have shown that celastrol can attenuate the proliferation and invasiveness of breast cancer cells by restraining the expression of interleukin-1β (IL-1β)[15]. Celastrol also suppresses the invasion of breast cancer cells by reducing the expression of matrix metalloproteinase 9 (MMP-9)[16]. Many studies have suggested that celastrol is a potential agent for the treatment of breast cancer; however, its targets in breast cancer inhibition remain unknown and the underlying mechanisms remain unclear. Quantitative chemical proteomics combining affinity chromatography and mass spectrometry (MS)

Li Liu and Yanqing Liu contributed equally to this work.

**Corresponding author. Jigang Wang, E-mail: jgwang@icmm.ac.cn; Yongping Zhu, E-mail: ypzhu@icmm.ac.cn.*

Received 14 August 2023 / Accepted 4 February 2024

How to cite this article: *Liu L, Liu YQ, Zhang SJ, Zhang JZ, Meng YQ, Liu DD, Gu LW, Zhang Y, Xu LT, Zhang ZY, Zhao MH, Wong YK, Wang QX, Zhu YQ, Wang JG. Celastrol promotes apoptosis of breast cancer MDA-MB-231 cells by targeting HSDL2. Acupunct Herb Med 2024;4(1):92–101. DOI: 10.1097/HM9.0000000000000102*

has been widely used to identify small molecule–protein interactions[17]. The identification of drug targets can deepen our understanding of the mechanism of action of celastrol and reveal its potential therapeutic applications and safety profile. In this study, we employed an activity-based celastrol probe (Cel-p) and quantitative chemical biology methods for target pull down and MS identification in breast cancer cells MDA-MB-231 to elucidate the anti-tumor targets and mechanisms of celastrol in MDA-MB-231 cells as a representative of TNBC.

Hydroxysteroid dehydrogenase-like 2 (HSDL2) belongs to the short-chain dehydrogenase/reductase (SDR) superfamily, which is located at the chromosome 9q32loci and is widely expressed in the liver, fat, and other tissues[18]. It catalyzes the reduction and oxidation of various substrates such as sugars, vitamin A, steroids, and fatty acids[19]. Studies have shown that HSDL2 is an effective regulator of fatty acid metabolism[20] and is abnormally expressed in numerous types of tumors. Although HSDL2 has been reported to play a role in the occurrence and development of breast cancer[21], few studies have investigated the role of HSDL2 in breast cancer, and its mechanism of action in the treatment of breast cancer remains unclear. Here, we found that HSDL2 was a direct target of celastrol in MDA-MB-231 cells. Additionally, celastrol inhibited HSDL2 expression and promoted apoptosis possibly *via* the mitogen-activated protein kinase (MAPK)/extracellular signal-regulated kinase (ERK) pathway.

Materials and methods

Reagents and antibodies

For drugs, MS-related reagents, and plasmid sequences, refer to literature[7,22]. The pCMV6-HSDL2 overexpression plasmid was purchased from OriGene. The antibodies used in the experiments are shown in Supplementary Table 1, http://links.lww.com/AHM/A100, and Supplementary Table 2, http://links.lww.com/AHM/A101.

Cell culture

The Union Medical College Cell Bank (Beijing, China) was used to obtain MDA-MB-231 cells. Cells were grown in RPMI-1640 (ThermoFisher, MA, USA) complemented with 10% fetal bovine serum (ThermoFisher) and 100 U/mL penicillin streptomycin solution (ThermoFisher) at 37°C and 5% CO_2. When the cells reached 80% to 90% confluence, they were passaged and frozen according to experimental requirements.

Cell viability assay

In a 96-well plate, 1×10^5 MDA-MB-231 cells were seeded for 20 hours before treatment with various celastrol doses (0, 0.0625, 0.125, 0.25, 0.5, 1, 2, 4, 8, and 16 μM) for 24 hours. Cells were then grown at 37°C and 5% CO_2 for 1 to 2 hours after being treated with 10 μL of cell counting kit-8 (CCK-8) assay buffer in 100 μL of media. A microplate reader (Thermo Fisher Scientific, Waltham, MA, USA) was used to analyze the 450 nm absorption spectra of each well.

Western blotting (WB)

Intracellular proteins were extracted using a lysis buffer containing protease inhibitors. Following quantification using the bicinchoninic acid assay, the samples were boiled and isolated using sodium dodecyl sulfate-polyacrylamide gel electrophoresis (SDS-PAGE), and the proteins were subsequently transferred to polyvinylidene fluoride (PVDF) membranes. After blocking with 5% bovine serum albumin (BSA) for 1 hour, membranes were incubated with specific secondary antibodies. Ultimately, an improved chemiluminescence plus detection device (Sapphire RGBNIR; Azure Biosystems, Dublin, CA, USA) was used to visualize the protein bands.

Cellular thermal shift assay (CETSA)

Cells diluted with double-distilled water (ddH_2O) containing 50 μM 4-hydroxyethyl piperazine ethanesulfonic acid (HEPES) pH 7.5, 100 μM Na_3VO_4, 10 mM $MgCl_2$, 1 mM TCEP, 5 mM β-glucuronidase, and 1× protease inhibitor, and stored in liquid nitrogen, were lysed through repeated freeze-thaw cycles. The supernatant was packaged into polymerase chain reaction (PCR) tubes and treated with celastrol (0, 5, 10, and 20 μM) for 1 h at room temperature. The solutions were heated in a thermocycler for 3 min at the stated temperatures (37°C, 52°C, and 56°C) and then cooled for 3 min at 4°C (Applied Biosystems, MA, USA). The soluble supernatant was analyzed using WB after centrifugation at 20,000×*g* for 25 min at 4°C.

Flow cytometry

Apoptosis was measured using the Apoptosis Detection Kit I for fluorescein isothiocyanate (FITC) Annexin V (Beyotime, Shanghai, China) according to the manufacturer's instructions. A BD LSRFortessa cell analyzer with Diva software (version 6.0) was used to collect data, and FlowJo software was used for additional analysis (BD Biosciences, Franklin Lake, NJ, USA).

Reverse transcription-PCR analysis

RNA was extracted using TRIzol reagent, chloroform, and isopropyl alcohol according to the manufacturer's guidelines. The amount of RNA was determined using a NanoDrop spectrophotometer (Thermo Fisher Scientific). RNA was converted to complementary DNA (cDNA) using a reverse transcription kit at the following temperatures: 25°C for 5 min, 50°C for 45 min, and 85°C for 5 min. Reverse transcription-PCR was used to amplify cDNA, according to the manufacturer's recommendations. Forty cycles of amplification were performed at the following temperatures: 94°C pre-denaturation for 30 seconds, 94°C denaturation for 5 seconds, 60°C annealing for 15 seconds, and 72°C extension for 10 seconds. The 2Ct technique was used to determine the mRNA expression of the target gene.

Fluorescence labeling

Six-well plates containing 6×10^5 cells were used to label the living cells *in situ*. After 80% to 90% confluence was achieved, Cel-p (0.5, 1, 2, and 4 μM) or dimethyl sulfoxide (DMSO) was added to the wells for 2 hours. Competitive trials to join the various celastrol incubation for 2 h. Cells were lysed using RIPA containing a 1× protease inhibitor. After protein measurement, 100 μg of protein (in 1 mM NaVC, 100 mM THPTA, 1 mM $CuSO_4$, and 50 mM TAMRA azide) was obtained for the click reaction. The reaction was allowed to proceed for 2 h at room temperature, with vigorous shaking. After overnight precipitation, the protein was separated by SDS-PAGE and 1× loading buffer (50 μL) was added. Visualization was accomplished using laser scanner fluorescence (Sapphire RGBNIR; Azure Biosystems). To determine the amount of protein loaded, SDS-PAGE gels were stained with the Instant Blue Coomassie Protein Stain.

Plasmid transfection

The plasmid was mixed with Lipofectamine 2000 (Thermo Fisher Scientific) in Opti-MEM (Thermo Fisher Scientific), according to the manufacturer's instructions. Subsequently, the cells were transfected with the mixture and cultured for 24 to 72 h according to experimental requirements.

Target identification

The experimental procedure was performed as previously described. In the presence or absence of the original drug (4×), the cells were treated for 4 h with Cel-p or DMSO, and the protein was extracted for the click reaction (biotin tag). After acetone precipitation, 1.5% SDS was added for ultrasonic rupture. Subsequently, 1× PBS (10.5 mL) was added and 1.5% SDS was diluted to 0.1%. The beads (60 μL) were then incubated at room temperature for 4 h. Thereafter, 1% SDS (30 mL; 10 mL each time) and 0.1% SDS (10 mL) were added. Protein samples incubated with beads were washed with 6 M urea (30 mL; 10 mL each time) and centrifuged at 1,000×*g* for 5 min at room temperature to remove nonspecific binding. Next, 100 mM dithiothreitol (25 μL) was added and the mixture was incubated at 37°C for 30 min on a shaker. Subsequently, 400 mM indole acetic acid (25 μL) was added and the mixture was incubated at 37°C for 50 min on a shaker. The mixture was washed three times with 1× PBS; 2 M urea (150 μL), 1 mM $CaCl_2$ (150 μL), and trypsin (2.5 μg) were added to each tube, and the mixture was incubated at 37°C overnight. To terminate the reaction, 0.1% formic acid was added to the digested samples. Subsequently, methanol (1 mL), acetonitrile (2 mL), and 0.1% formic acid in water (3 mL) were added to activate the column. The supernatant samples were loaded five times, along with 0.1% formic acid water (2 mL) for desalting and formic acid water 70% acetonitrile (500 μL). The 1 M tetraethyl-ammonium bromide (TEAB) was diluted to 100 mM with ddH_2O, and the dried protein sample was re-dissolved in 20 μL TEAB. Four microliters of different tandem mass tag (TMT) reagents (128C, 130N, and 127C) were added to each group and labeled. Samples were incubated in a shaker at 37°C and 800 rpm for 2 hours in the dark. After the reaction was completed, 20 μL of 1 M Tris-HCl (pH = 8.0) was added to each tube to terminate the reaction. The three tubes were then combined into one tube for desalination (the steps were the same as above). The eluted sample was dried and frozen at −80°C for long-term storage. Dried samples were re-suspended in 0.1% formic acid in water and 1% acetonitrile for liquid chromatography-tandem mass spectrometry (LC-MS/MS) analysis.

Cellular imaging

Cells were plated in a confocal dish and incubated with Cel-p for different time periods (0, 60, and 120 min). Cells were washed three times with 1× PBS, fixed with 4% paraformaldehyde for 20 min, washed three times with 1× PBS, incubated with 0.2% TitonX-100 for 15 min for permeabilization, washed three times with 1 ×PBS, blocked with 5% BSA for 1 h, washed three times with 1× Tris buffered saline Tween (TBST), and incubated with click reagent for 2 h in the dark. The freshly prepared click reaction reagent was incubated with the cells for 2 h at room temperature with gentle shaking. The cells were then washed three times with 1× TBST.

Statistical analysis

In all statistical analyses in this study, $P < 0.05$ indicated that the difference was statistically significant, and the experimental data are presented as mean ± standard error (X ± SEM). SPSS (version 26.0) was used as the statistical analysis software and GraphPad prism 8.0 was used as the mapping software.

Results

The targets of celastrol in MDA-MB-231 cells were identified by ABPP

A modified celastrol was synthesized and termed Cel-p (Figure 1A). In the synthesis of Cel-p, we introduced an alkyne group far from the active center of celastrol, which was unlikely to destroy its bioactivity (Figure 1A). The CCK-8 assay was used to determine whether celastrol and Cel-p exhibited similar cytotoxicity and the most effective drug concentration. The results showed that the half maximal inhibitory concentration (IC_{50}) values of Cel-p and celastrol were 1.973 and 1.445 μM, respectively (Figure 1B). These data indicated that celastrol and Cel-p exhibited similar cytotoxicities, confirming the equivalence of the probe and the original drug. Celastrol had a concentration-dependent ability to significantly reduce cell viability and proliferation at concentrations greater than 1.973 μM. Therefore, the probe synthesized by introducing a bioorthogonal reaction group into celastrol did not affect the activity of the original drug, and Cel-p could be used in subsequent research. These results indicate that the anti-cancer activity of celastrol was completely retained in the modified molecule.

The fluorescent dye or biotin tag was added to the alkyne group *via* a click chemistry reaction, allowing

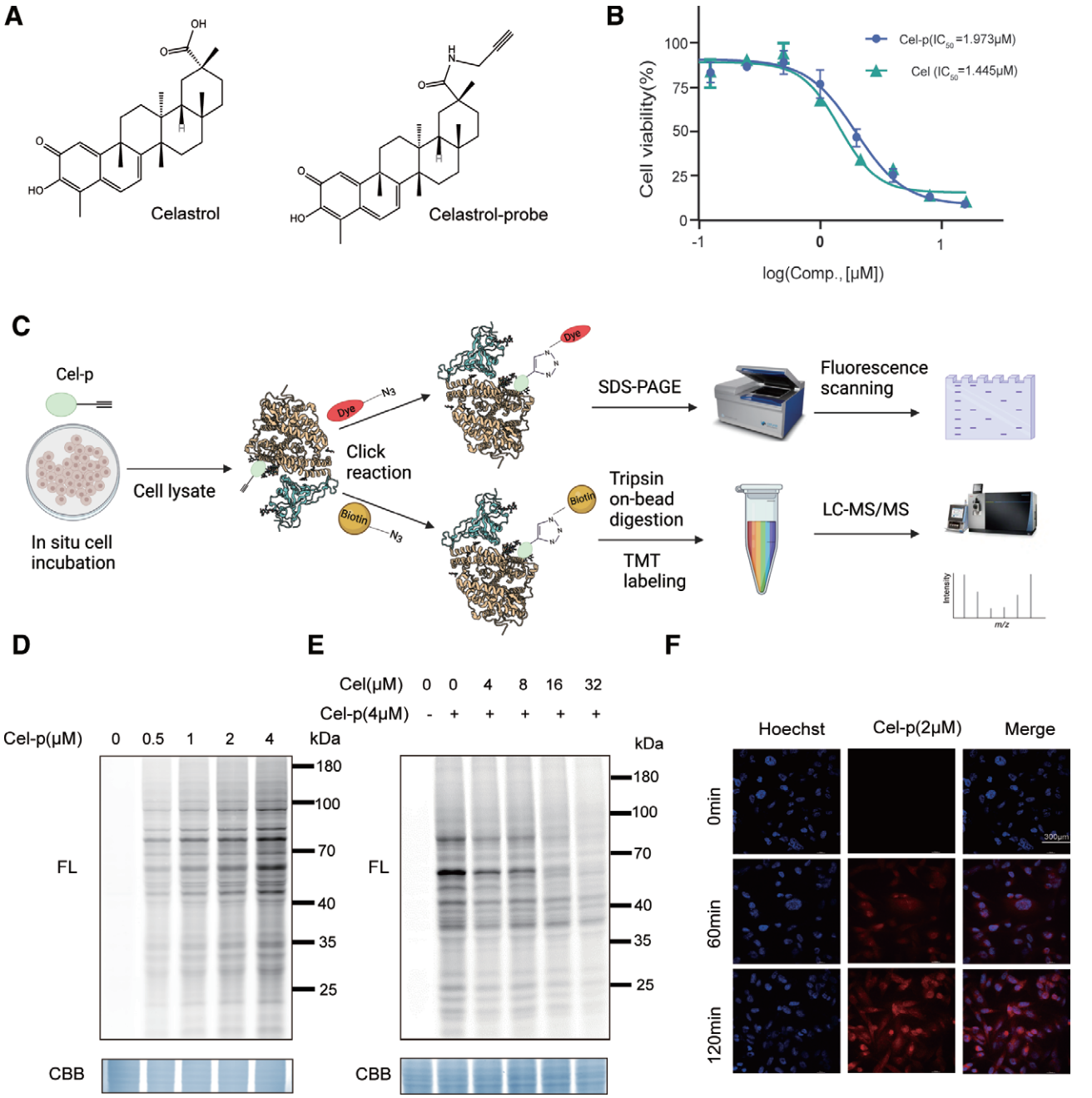

Figure 1. The targets of Cel in the MDA-MB-231 cells were identified using ABPP. (A) Chemical structures of Cel and Cel-P. (B) IC_{50} values of Cel and Cel-p in MDA-MB-231 cells. (C) Process flow for identifying possible Cel targets by ABPP profiling. (D) Labeling efficiency of Cel-p in living cells at concentrations of 0–4 μM. (E) Competitive effect of Cel-p on living cells during early incubation with Cel (1×, 2×, 4×, and 8×). (F) Cellular imaging of Cel-p in MDA-MB-231 cells (scale bar: 300 μm). ABPP: Activity-based protein profiling; CBB: Coomassie brilliant blue; Cel: Celastrol; Cel-p: Celastrol probe; FL: Fluorescence; IC_{50}, Half maximal inhibitory concentration; LC-MS/MS: Liquid chromatography-tandem mass spectrometry; SDS-PAGE: Sodium dodecyl sulfate-polyacrylamide gel electrophoresis; TMT: Tandem mass tag.

the targets of Cel-p to be visualized by SDS-PAGE or affinity-purified targets identified by MS (Figure 1C). We investigated the effectiveness of Cel-p protein labeling and competition efficiency with celastrol to determine the possible target proteins of celastrol. As shown in Figure 1D, after 4 hours of incubation with Cel-p at a concentration of 4 μM, strong labeling efficiency and concentration-dependent labeling of MDA-MB-231 cells and obviously visible bands were observed. The labeling efficiency of Cel-p (4 μM) became progressively weaker under the condition with the celastrol competitor (4-32 μM), suggesting that the probe bound similar target proteins to those of celastrol (Figure 1E). Subsequently, the Cel-p alkyne tag was used to perform a click chemistry reaction with the red fluorescent dye tetramethylrhodamine (TAMRA) azide to detect its subcellular localization. Cell imaging showed that Cel-p entered the nucleus from the cytoplasm after 2 h (Figure 1F). These data indicated that Cel-p had a high labeling efficiency *in vitro* and could be used in subsequent chemical proteomic analyses.

Celastrol promoted apoptosis of MDA-MB-231 cells

Previous studies have indicated that treatment with celastrol can induce apoptosis in cancer cells[11,23].

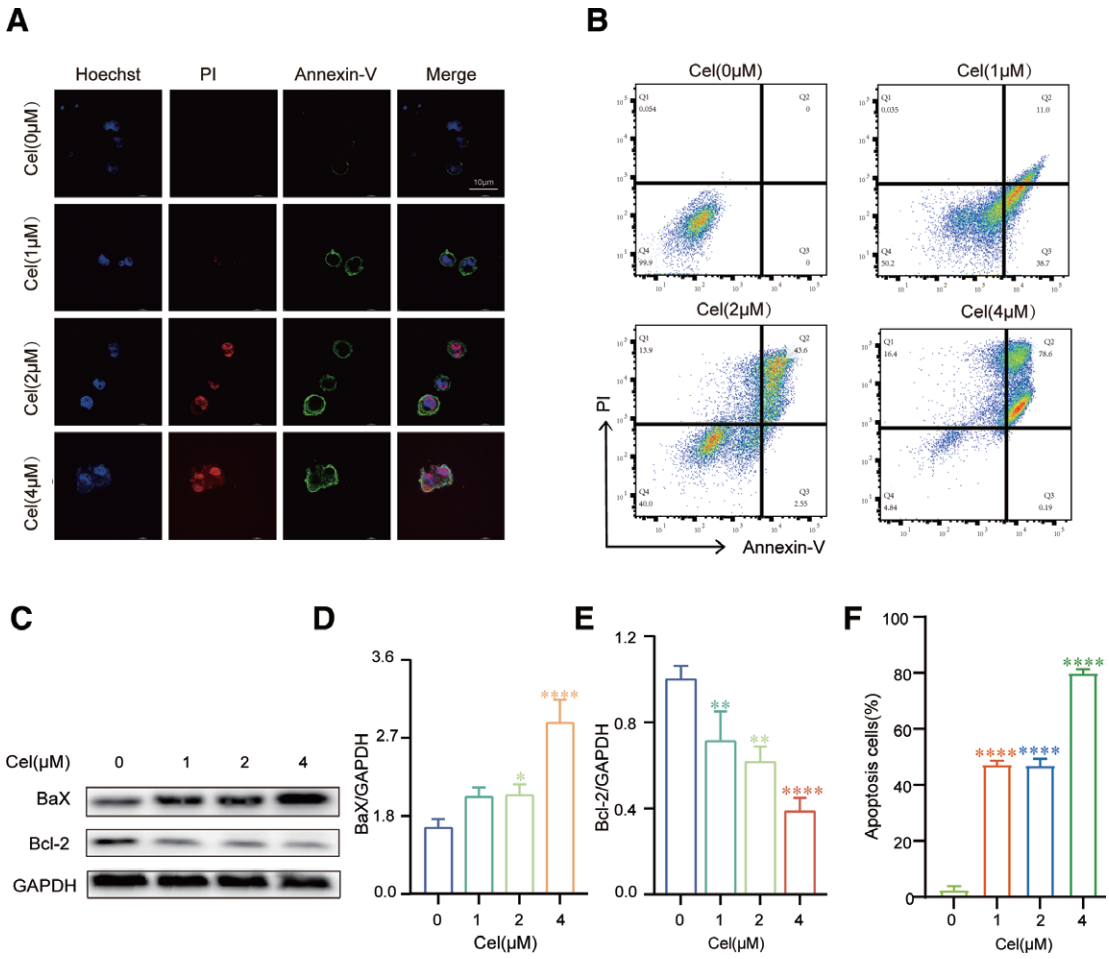

Figure 2. Celastrol promotes apoptosis in breast cancer cells. (A) Fluorescence intensity analysis after incubation of MDA-MB-231 cells with Hoechst 33342/Annexin V-FITC/PI (scale bar: 10 μm). (B, F) Apoptosis was detected using flow cytometry. Data are presented as the mean ± SD ($n = 3$). *$P < 0.05$, **$P < 0.01$, ****$P < 0.0001$ denote statistically significant differences compared with the control group. (C–E) BaX and Bcl-2 levels were measured by WB. GAPDH was used as a loading control. BaX: Bcl-2-associated X; Bcl-2: B-cell lymphoma-2; FITC: Fluorescein isothiocyanate; GAPDH: Glyceraldehyde-3-phosphate dehydrogenase; PI: Propidium iodide; SD: Standard deviation; WB: Western blotting.

Here, we investigated whether celastrol induces apoptosis in MDA-MB-231 cells and explored the underlying molecular mechanisms. Cells were treated with celastrol (1, 2, and 4 μM) or DMSO, and apoptosis was detected by flow cytometry analysis using Annexin V-FITC/propidium iodide (PI) staining. As shown in Figure 2A, the PI red probe accumulated in the nucleus and emitted a strong red fluorescent signal in the drug groups, the Annexin V green fluorescence was significantly reinforced only in the cytoplasm, and the cell membrane ruptured in the celastrol group (4 μM). The results showed that apoptosis was concentration-dependent, where only early apoptosis occurred at 1 μM celastrol and late apoptosis began to occur when the concentration was increased to 2 μM (Figure 2B, F). B-cell lymphoma-2 (Bcl-2) and Bcl-2-associated X (BaX) are typical biomarkers of the mitochondrial apoptosis pathway. Therefore, we detected changes in Bcl-2 and BaX levels using WB as indicators of celastrol-induced apoptosis (Figure 2C). The results showed that compared to the control group (0 μM), the expression levels of BaX and Bcl-2 in the celastrol group increased and decreased, respectively (Figure 2D, E). These results revealed that celastrol induces apoptosis in MDA-MB-231 cells in a dose-dependent manner.

Celastrol directly bound to HSDL2

TMT-labeled quantitative chemical proteomics was used to identify the Cel-p targets in MDA-MB-231 cells. Cells were incubated with Cel-p (4 μM) in the presence or absence of celastrol (16 μM) for 4 hours. Cell lysates were then incubated with streptavidin beads, which can be used to collect labeled proteins. Subsequently, the samples were subjected to denaturation, reduction, and digestion, and the peptides were identified by LC-MS/MS. A total of 828 targets were identified. Based on the ratios of the probe and competitive groups (>2 and >1, respectively), 41 of these proteins were found to be highly reliable (Figure 3A). HSDL2 was identified as a direct binding target of celastrol, and previous studies have demonstrated its role in tumors[24]. Therefore, we further investigated the importance of HSDL2. The pull-down assay and WB were performed to verify direct interactions between celastrol and HSDL2. The results showed that celastrol (4×) completely competed for binding of Cel-p to HSDL2, indicating that HSDL2 directly interacted with celastrol (Figure 3B). The results of the CETSA further supported the idea that the direct interaction between celastrol and HSDL2 increased the thermal stability of the latter compared to that of the control group (Figure 3C, D).

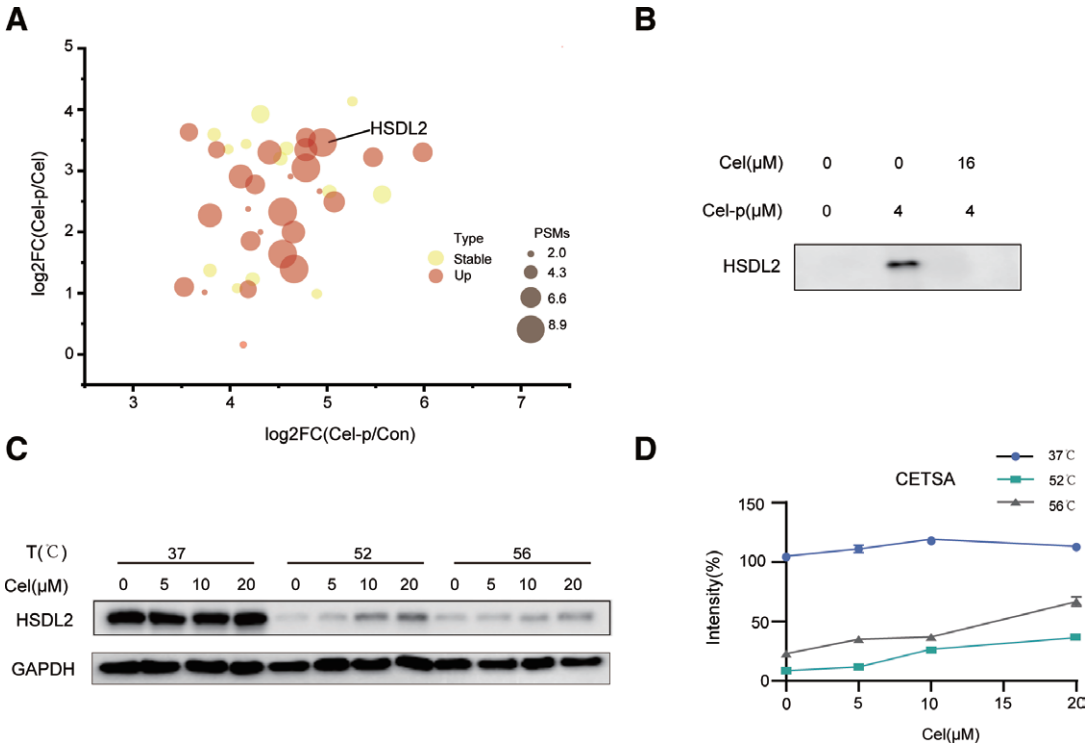

Figure 3. Cel bounds directly to HSDL2. (A) After treatment with Cel-p (4 μM) and Cel (16 μM), 828 targets were captured by ABPP and mass spectrometry. The high-confidence target was HSDL2. The following criteria were established: 41 measured proteins from the Cel-P ABPP experiment are shown in a scatter plot. The x-axis shows the mean log2 difference in protein abundance between the Cel-p and DMSO control groups, while the y-axis shows the mean log2 difference between the Cel-p and Cel + Cel-p groups. Each dot represents the measured protein. The associated number of peptide spectrum matches was inversely correlated with the dot size. (B) Pull-down western blotting revealed that Cel-P and Cel had the same binding ability to HSDL2. (C, D) CETSA revealed that Cel binds to HSDL2 and improves its thermal stability. For HSDL2, whole cell lysates were analyzed. GAPDH was used as a loading control. ABPP: Activity-based protein profiling; Cel: Celastrol; Cel-P: Celastrol probe; CETSA: Cellular thermal shift assay; DMSO: Dimethyl sulfoxide; FC: Fold change; GAPDH: Glyceraldehyde-3-phosphate dehydrogenase; HSDL2: Hydroxysteroid dehydrogenase-like 2; PSMs: Peptide-spectrum matches.

HSDL2 affected the apoptosis of MDA-MB-231 cells

To further investigate the relationship between HSDL2 and apoptosis in MDA-MB-231 cells, we used transient transfection to knock down the expression of HSDL2. WB and quantitative polymerase chain reaction (qPCR) analyses confirmed that the expression of HSDL2 decreased at both the protein and mRNA levels (Figure 4B, C). Moreover, the expression of the pro-apoptotic protein BaX increased, whereas that of the anti-apoptotic protein Bcl-2 decreased (Figure 4B). The results of flow cytometry analysis showed that the apoptosis rate increased, thereby confirming that the knockdown of HSDL2 expression promoted apoptosis (Figure 4A). Moreover, it also reduced the IC_{50} value of celastrol (Figure 4D). Contrastingly, overexpression of HSDL2 in cells resulted in the opposite effects, and apoptosis was reversed (Figure 4E–H). These data suggested that HSDL2 mediates apoptosis in breast cancer cells.

Celastrol promoted apoptosis of MDA-MB-231 cells by targeting HSDL2

Previous studies have confirmed that celastrol can induce apoptosis and that knockdown of HSDL2 promotes apoptosis. However, it remains unclear whether celastrol induces apoptosis by acting on HSDL2. Initially, the expression of HSDL2 was measured after treatment with different drug concentrations and at various time points after *in situ* administration. The results showed that HSDL2 expression decreased in a concentration- and time-dependent manner (Figure 5A, B). Subsequently, we measured the expression levels of the BaX and Bcl-2 proteins after celastrol treatment and HSDL2 overexpression. After overexpression of HSDL2, the expression of the pro-apoptotic protein BaX decreased, whereas that of the anti-apoptotic protein Bcl-2 increased compared to that in the control group (Figure 5C). Collectively, these results reveal that celastrol targets HSDL2 and effectively inhibits its expression, thereby inducing apoptosis in breast cancer cells.

Celastrol inhibited the phosphorylation of the MAPK pathway in MDA-MB-231 cells

We demonstrated that celastrol promoted apoptosis by inhibiting the expression of HSDL2. To further understand the mechanism of this action, we conducted an in-depth study of the signaling pathways related to HSDL2. It has been reported that the inhibition of HSDL2 could be carried out by suppressing the ERK pathway[24]. According to the Kyoto Encyclopedia of Genes and Genomes pathway analysis, our differentially expressed proteins were mainly related to the MAPK cascades, which participate in the regulation of apoptosis in tumor cells and form a classical signal transduction signaling pathway with ERK[25] (Figure 6A). Therefore, we investigated whether celastrol influences the MAPK/ERK pathway by inhibiting ERK phosphorylation. As shown in Figure 6B, ERK phosphorylation was inhibited after treatment with celastrol in a

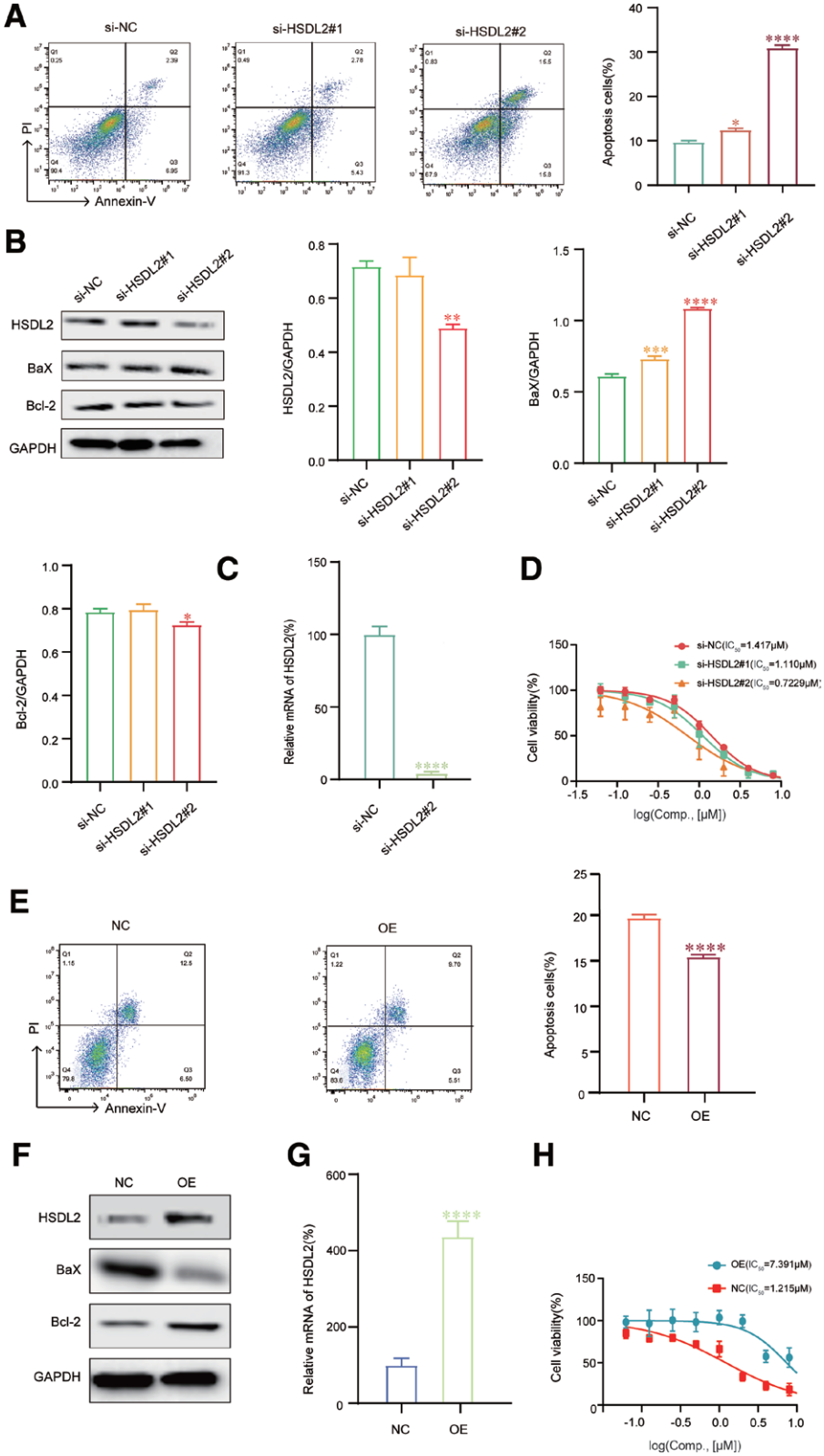

Figure 4. HSDL2 affects breast cancer cell apoptosis. HSDL2 knockdown by siRNA transfection in MDA-MB-231 cells. (siRNA: si-HSDL2#1 or si-HSDL2#2; NC: negative control siRNA; $n = 3$.) (A–D) Flow cytometry, estern blotting, qPCR, and CCK-8 assays were used to detect the effect of HSDL2 knockdown on apoptosis. GAPDH was used as a loading control. (E–H) Flow cytometry, western blotting, qPCR, and CCK-8 assays were used to detect the effect of HSDL2 protein overexpression on apoptosis. GAPDH was used as a loading control. Data are shown as mean SD ($n = 3$) of the total data. The following symbols indicate statistically significant differences from the control group: *$P < 0.05$, **$P < 0.01$, ***$P < 0.001$, ****$P < 0.0001$. BaX: Bcl-2-associated X; Bcl-2: B-cell lymphoma-2; CCK8: Cell counting kit-8; GAPDH: Glyceraldehyde-3-phosphate dehydrogenase; HSDL2: Hydroxysteroid dehydrogenase-like 2; OE: Overexpression; PI: Propidium iodide; qPCR: Quantitative polymerase chain reaction; SD: Standard deviation; siRNA: Small interfering RNA.

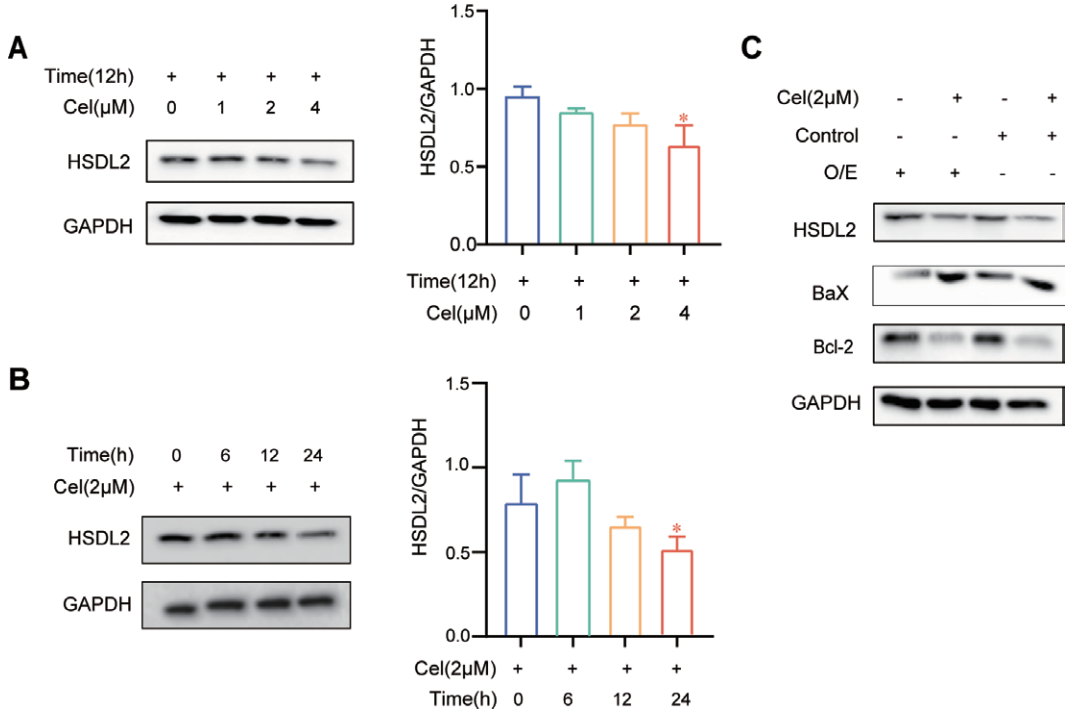

Figure 5. Celastrol promotes the apoptosis of breast cancer cells by acting on HSDL2. (A, B) After treatment with various doses of celastrol (0, 1, 2, 4 μM) and at various intervals (0, 6, 12, 24 h), the expression of HSDL2 was detected by using WB. (C) The levels of HSDL2 and apoptotic proteins were detected by WB after the administration of celastrol in the control and overexpression groups. *$P < 0.05$. BaX: Bcl-2-associated X; Bcl-2: B-cell lymphoma-2; GAPDH: Glyceraldehyde-3-phosphate dehydrogenase; HSDL2: Hydroxysteroid dehydrogenase-like 2; O/E: Overexpression; WB: Western blotting.

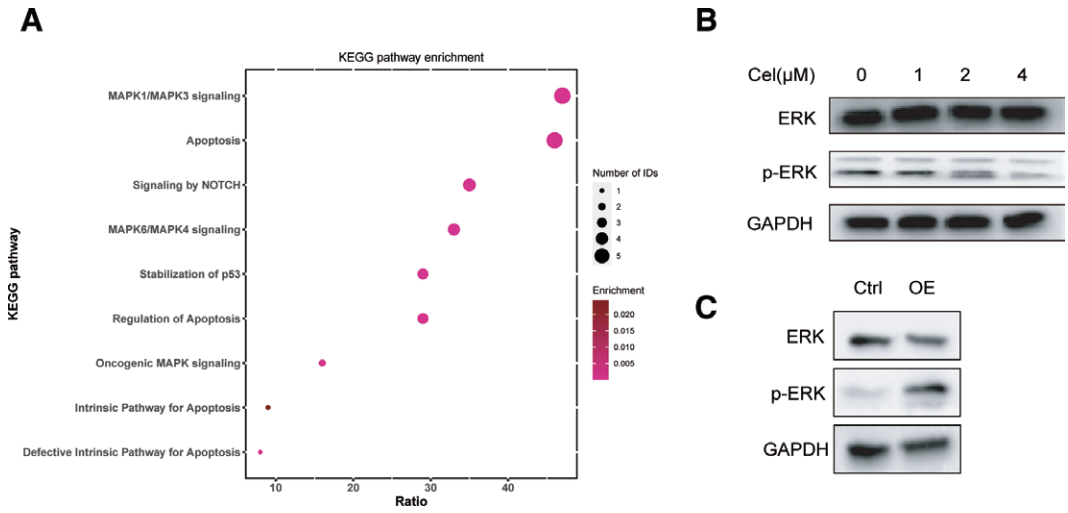

Figure 6. In MDA-MB-231 cells, celastrol inhibits the MAPK pathway. (A) Mass spectrometry data were imported into the DAVID database and nine high-confidence pathways were identified. (B, C) The protein expressions of ERK and p-ERK were detected by WB after 24 h of celastrol administration (0, 1, 2, 4 μM) or 48 h of HSDL2 overexpression. ERK: Extracellular signal-regulated kinase; GAPDH: Glyceraldehyde-3-phosphate dehydrogenase; HSDL2: Hydroxysteroid dehydrogenase-like 2; KEGG: Kyoto encyclopedia of genes and genomes; MAPK: Mitogen-activated protein kinase; OE: Overexpression; p-ERK: Phosphorylated extracellular signal-regulated kinase; WB: Western blotting.

concentration-dependent manner. Following overexpression of HSDL2, the phosphorylation level of ERK significantly increased (Figure 6C). These results revealed that celastrol induced apoptosis by suppressing the HSDL2/MAPK/ERK signaling pathway.

Discussion

Breast cancer is a common cause of mortality in females in developing countries[26]. Compared to other types of breast cancer, TNBC is characterized by strong invasiveness, difficult diagnosis, high metastatic potential, and poor response to endocrine and targeted therapies. Therefore, it is necessary to develop novel therapeutic strategies for TNBC. Celastrol is a pentacyclic triterpenoid compound that has been reported to be effective in treating breast cancer; however, the targets of celastrol in breast cancer inhibition are still unknown, and the underlying mechanisms remain unclear. Here, we investigated the direct interaction targets of celastrol in MDA-MB-231 cells and found that HSDL2 is a specific binding target of celastrol and celastrol-mediated apoptosis *via* the HSDL2/MAPK/

ERK pathway in MDA-MB-231 cells. These findings provide new directions for breast cancer research and clinical treatment of TNBC. However, it may also exert antitumor effects through other target proteins or signaling pathways, and more in-depth studies are needed.

To investigate the fundamental mechanisms and target proteins of celastrol in breast cancer cells, Cel-p was created using a clickable alkyne tag. Subsequently, the target protein covalently bound to celastrol was identified using a combination of activity-based protein profiling (ABPP), biological orthogonal clicking chemistry, and LC-MS/MS. The results of the ABPP assay indicated that celastrol directly binds to HSDL2. HSDL2 is responsible for steroid hormone biosynthesis in cells. Studies have shown that HSDL2 is involved in lipid metabolism and regulates the growth, proliferation, and metastasis of cervical cancer cells[22]. Currently, only the natural drug, cucurbitacin E, has been shown to inhibit the expression of HSDL2 in tumor cells[24]. We used synthetic Cel-p to label and compete with the original drug protein *in situ* and the results identified HSDL2 as one of the most reliable targets. The pull-down assay and CETSA WBs also clearly demonstrated that celastrol targeted HSDL2. Following *in situ* administration, celastrol inhibited HSDL2 expression in a concentration-dependent manner.

Apoptosis plays a significant role in the maintenance of cellular homeostasis during normal development and aging[27]. In type I programmed apoptosis, cells exhibit obvious characteristic changes, cell contracture after the nucleus, cytoplasmic fragmentation, and cell membrane blistering; finally, the formed apoptotic bodies are phagocytosed[28]. The Bcl-2 family of genes is mainly located in the mitochondrial membrane of cells. BaX can form a dimer with Bcl-2, inhibit the activity of Bcl-2, and prevent the passage of cytochrome C through the mitochondria[29,30]. We confirmed that celastrol treatment promoted apoptosis in MDA-MB-231 cells. Moreover, the expression of the pro-apoptotic protein BaX increased, that of the anti-apoptotic protein Bcl-2 decreased, and the rate of apoptosis increased. After the knockdown of HSDL2 in MDA-MB-231 cells, the apoptosis rate was similar to that observed after celastrol administration. However, apoptosis was reversed by the overexpression of HSDL2. These results suggest that celastrol promotes apoptosis by inhibiting HSDL2 expression.

To further understand the underlying mechanism of this action, we conducted an in-depth study of the signaling pathways related to HSDL2. Our MS data showed that the differentially expressed proteins were mainly related to the MAPK cascades that participate in the regulation of apoptosis in tumor cells and form a classical signal transduction signaling pathway with ERK. The inhibition of HSDL2 could also be carried out by suppressing the ERK pathway[24]. Therefore, we examined whether celastrol inhibits HSDL2 expression and induces apoptosis in cancer cells through the MAPK/ERK signaling pathway.

The rapidly accelerated fibrosarcoma (RAF)-MEK-ERK signaling cascade is a well-characterized MAPK pathway involved in cell proliferation and survival[31]. ERKs (ERK1 and ERK2), also termed MAPK3 and MAPK1, respectively[32], are downstream signaling modules that initiate a three-layer MAPK signaling cascade after the activation of receptor tyrosine kinase (RTK) and reliability, availability and serviceability (RAS), thereby guiding a series of physiological functions[33]. Abnormal activation of the MAPK1/3 pathway is associated with tumor development[34,35]. Therefore, we selected ERK molecules in the MAPK pathway to verify whether celastrol and HSDL2 were involved in the MAPK1/3 pathway. ERK phosphorylation in the MAPK pathway changed after celastrol administration and HSDL2 overexpression. Thus, our results confirm that celastrol is involved in the regulation of the MAPK1/3 pathway through HSDL2. Based on these results, we concluded that celastrol induces apoptosis by suppressing the HSDL2/MAPK/ERK signaling pathway. Our results provide new binding targets for celastrol in the treatment of cancer as well as additional agent options and target information for the treatment of breast cancer, especially TNBC.

Conflict of interest statement

The authors declare no conflict of interest.

Funding

The following financing sources are acknowledged for their assistance: the National Key Research and Development Program of China (2020YFA0908000 and 2022YFC2303600), the National Natural Science Foundation of China (81903866 and 82274182), and the Central Public Welfare Research Institutes (ZZ13-YQ-105; ZZ15-YQ-065; ZZ14-YQ-058).

Author contributions

The experiments were created by Jigang Wang and Yongping Zhu, who also oversaw the initiative. The main experiments, paper writing, and data analysis were done by Liu Li and Yanqing Liu. Shujie Zhang, Liting Xu, Ziyue Zhang, Minghong Zhao, and Qixin Wang helped with *in vitro* experiments. Liwei Gu, Dandan Liu, and Yuqing Meng revised the manuscript. Junzhe Zhang and Ying Zhang performed mass spectrometry experiments. The final manuscript was reviewed and approved by all authors.

Ethical approval of studies and informed consent

Written informed consent for publication of this paper was obtained from the Gannan Medical University of Arts and Science and all authors.

Acknowledgments

We appreciate the contributions made to this continually developing area of celastrol study by our coworkers, colleagues, and laboratory staff.

Data availability statement

All data associated with this study are present in the paper or the Supplementary Materials.

References

[1] Sung H, Ferlay J, Siegel RL, et al. Global cancer statistics 2020: GLOBOCAN estimates of incidence and mortality worldwide for 36 cancers in 185 countries. *CA Cancer J Clin* 2021;71(3):209–249.

[2] McGuire S. World Cancer Report 2014. Geneva, Switzerland: World Health Organization, International Agency for Research on Cancer, WHO Press 2015. *Adv Nutr* 2016;7(2):418–419.

[3] Dhakal R, Noula M, Roupa Z, et al. A scoping review on the status of female breast cancer in Asia with a special focus on Nepal. *Breast Cancer (Dove Med Press)* 2022;14:229–246.

[4] Dent R, Trudeau M, Pritchard KI, et al. Triple-negative breast cancer: clinical features and recurrence patterns. *Clin Cancer Res* 2007;13(15 Pt 1):4429–4434.

[5] Mezni E, Behi K, Goncalves A. Immunotherapy and breast cancer: an overview. *Curr Opin Oncol* 2022;34(5):587–594.

[6] Pace S, Zhang K, Jordan PM, et al. Anti-inflammatory celastrol promotes the switch from leukotriene biosynthesis to the formation of specialized pro-resolving lipid mediators. *Pharmacol Res* 2021;167:105556.

[7] Liu DD, Luo P, Gu L, et al. Celastrol exerts a neuroprotective effect by directly binding to HMGB1 during cerebral ischemia-reperfusion. *J Neuroinflammation* 2021;18(1):174.

[8] Feng X, Guan D, Auen T, et al. IL1R1 is required for leptin sensitization and the anti-obesity effects of celastrol. *Nat Med* 2019;25(4):575–582.

[9] Zhu C, Yang J, Zhu Y, et al. Celastrol alleviates comorbid obesity and depression by directly binding to amygdala HnRNPA1 in a mouse model. *Clin Transl Med* 2021;11(6):e394.

[10] Chen G, Zhu X, Li J, et al. Celastrol inhibits lung cancer growth by triggering histone acetylation and acts synergistically with HDAC inhibitors. *Pharmacol Res* 2022;185:106487.

[11] Chen X, Zhao Y, Luo W, et al. Celastrol induces ROS-mediated apoptosis by directly targeting peroxiredoxin-2 in gastric cancer cells. *Theranostics* 2020;10(22):10290–10308.

[12] Kun-Ming C, Chih-Hsien C, Chen-Fang L, et al. Potential anticancer effect of celastrol on hepatocellular carcinoma by suppressing CXCR4-related signal and impeding tumor growth in vivo. *Arch Med Res* 2020;51(4):297–302.

[13] Zhang J, Wang R, Cheng L, et al. Celastrol inhibits the proliferation, invasion, and migration of human cervical HeLa cancer cells through the downregulation of MMP-2 and MMP-9. *J Cell Mol Med* 2021;25(11):5335–5338.

[14] Liu Z, Fan M, Xuan X, et al. Celastrol inhibits migration and invasion and enhances the anticancer effects of docetaxel in human triple-negative breast cancer cells. *Med Oncol* 2022;39(12):189.

[15] You D, Jeong Y, Yoon SY, et al. Celastrol attenuates the inflammatory response by inhibiting IL-1beta expression in triple-negative breast cancer cells. *Oncol Rep* 2021;45(6):89.

[16] Kim Y, Kang H, Jang SW, et al. Celastrol inhibits breast cancer cell invasion via suppression of NF-κB-mediated matrix metalloproteinase-9 expression. *Cell Physiol Biochem* 2011;28(2):175–184.

[17] Wang J, Gao L, Lee YM, et al. Target identification in natural and traditional medicines using quantitative chemical proteomic approaches. *Pharmacol Ther* 2016;162:10–22.

[18] Han A, Xu R, Liu Y, et al. HSDL2 acts as a promoter in pancreatic cancer by regulating cell proliferation and lipid metabolism. *Onco Targets Ther* 2021;14:435–444.

[19] Kowalik D, Haller F, Adamski J, et al. We determined the functions of the two human orphan SDR enzymes, hydroxysteroid dehydrogenase-like 2 (HSDL2) and short-chain dehydrogenase/reductase-orphan (SDR-O). *J Steroid Biochem Mol Biol* 2009;117(4-5):117–124.

[20] Yu Y, Ge X, Wang LS, et al. Abnormalities in hsa-mir-16 and hsa-mir-124 affect mitochondrial function and fatty acid metabolism in tetralogy of Fallot. *Comb Chem High Throughput Screen* 2023;26(2):373–382.

[21] Dong B, Yang Y, Han A, et al. Ectopic HSDL2 expression is associated with breast cancer cell proliferation and prognosis. *Cancer Manag Res* 2019;11:6531–6542.

[22] Yang Y, Han A, Wang X, et al. Lipid metabolism regulator human hydroxysteroid dehydrogenase-like 2 (HSDL2) modulates cervical cancer cell proliferation and metastasis. *J Cell Mol Med* 2021;25(10):4846–4859.

[23] Mi C, Shi H, Ma J, et al. Celastrol induces apoptosis of breast cancer cells and inhibits their invasion via downregulation of MMP-9. *Oncol Rep* 2014;32(6):2527–2532.

[24] Liu WB, Wang HL, Chen L, et al. Cucurbitacin E inhibits cellular proliferation and induces apoptosis in melanoma cells by suppressing HSDL2 expression. *Chin Med* 2022;17(1):28.

[25] Guo YJ, Pan WW, Liu SB, et al. The ERK/MAPK signalling pathway and tumorigenesis. *Exp Ther Med* 2020;19(3):1997–2007.

[26] Umer M, Naveed M, Alrowais F, et al. Breast cancer detection using convoluted features and ensemble machine learning algorithm. *Cancers (Basel)* 2022;14(23):6015.

[27] Cosentino K, Garcia-Saez AJ. Mitochondrial alterations during apoptosis. *Chem Phys Lipids* 2014;181:62–75.

[28] Abdulhussein D, Kanda M, Aamir A, et al. Apoptosis in healthy and diseased eyes and brain. *Adv Protein Chem Struct Biol* 2021;126:279–306.

[29] Dadsena S, Zollo C, Garcia-Saez AJ. Mechanisms of mitochondrial cell death. *Biochem Soc Trans* 2021;49(2):663–674.

[30] Tait SW, Green DR. Mitochondria and cell death: outer membrane permeabilization and beyond. *Nat Rev Mol Cell Biol* 2010;11(9):621–632.

[31] Asl ER, Amini M, Najafi S, et al. Interplay between the MAPK/ERK signaling pathway and miRNAs: a crucial mechanism regulating cancer cell metabolism and tumor progression. *Life Sci* 2021;278:119499.

[32] Roskoski R. ERK1/2 MAP kinases: structure, function, and regulation. *Pharmacol Res* 2012;66(2):105–143.

[33] Ullah R, Yin Q, Snell AH, et al. RAF-MEK-ERK pathway in cancer evolution and treatment. *Semin Cancer Biol* 2022;85:123–154.

[34] Deng R, Zhang HL, Huang JH, et al. MAPK1/3 kinase-dependent ULK1 degradation attenuates mitophagy and promotes bone metastasis in breast cancer. *Autophagy* 2021;17(10):3011–3029.

[35] Ramirez-Ardila D, Timmermans AM, Helmijr JA, et al. Increased MAPK1/3 phosphorylation in luminal breast cancer related with PIK3CA hotspot mutations and prognosis. *Transl Oncol* 2017;10(5):854–866.